Development of a systematic design process for electrified drive systems and its validation based on an electrified drive axle for a heavy commercial vehicle

Roland Uerlich[1], Sven Köller[1], Gordon Witham[1], Theo Koch[1], Lutz Eckstein[1]

[1] *Institute for Automotive Engineering (ika), Steinbachstr. 7, 52074 Aachen, Germany,*
office@ika.rwth-aachen.de

Summary

The transport of goods accounts for about half of all the distances travelled in Europe. Hence, freight transport is one of the critical factors for reducing greenhouse gases and air pollutants. For this reason, the electrification of road freight transport is being pursued within the 'BEV Goes eHighway – [BEE]' project. The data basis for the modelling used in this project is provided by an electric drive axle for a heavy commercial vehicle developed in the project 'Concept-ELV²'. Using the results of the previous project as an example, this paper presents the developed methodological tools. The drive axle used as an example in this paper was specially designed for heavy urban delivery traffic, which is characterised by the wide range of performance requirements. Therefore, switchable transmission elements have been integrated within the powertrain to optimise the overall efficiency.

Keywords: electric powertrain, heavy duty, Holistic powertrain design, modular topology

1   Introduction

For the evaluation of commercial vehicle-related emissions, a standardized Europe-wide tool was developed in 2018 in the form of VECTO (Vehicle Energy Consumption Calculation Tool). As is already customary for the passenger car segment with the WLTP (Worldwide harmonized Light vehicles Test Procedure), this tool defines reference cycles, test procedures and their boundary conditions, as well as the recording of emission values in real road traffic [1]. Since the segment of heavy-duty commercial vehicles covered by VECTO comprises fewer units but a significantly higher number of variants, component tests are used more frequently in this procedure [2]. These also enable less common vehicle variants to be evaluated concerning their emissions without an individual test procedure using standardized longitudinal dynamic simulation models. In this approach, transverse dynamic effects are neglected, as they have only a small impact on vehicle efficiency.

In the current certification processes, battery-electric vehicles are considered zero-emission vehicles both in the commercial and passenger car sectors, as they do not exhaust any local CO2 emissions. Thus, even a small number of these vehicles has a significant impact on the fleet footprint of a vehicle manufacturer. However, this approach neglects the preceding process of energy generation, which also disregards the efficiency of the energy

use of the respective vehicles. As a result, this factor, which is crucial for the success of the technology change, is only of secondary importance. [3]

Consequently, the current legislative situation is similar to the situation in the entire commercial vehicle sector before the introduction of the VECTO, as no standardized approaches are currently defined to assess the efficiency of a commercial electric vehicle. As this topic has the previously described significant influence on the success of the technology and is gaining in importance due to the new regulatory environment, the first approaches for a supplement to the VECTO have already been developed. These are currently being implemented in a binding form [4,5].

2   General Methodology

In order to meet the challenges of electrifying powertrains, a tool was expanded and applied within the 'Concept-ELV²' project that was developed at the Institute for Automotive Engineering (ika) for the synthesis and design of powertrains [6]. The holistic approach chosen starts with the basic parameters of the vehicle and derives component-centred requirements using longitudinal dynamic vehicle models. This systematic assessment of the individual component requirements enables the optimization of each individual component and the simultaneous modelling of the interdependencies between those components. One reason is that each powertrain component's individual optimum does not often lead to the optimum within the entire powertrain [7]. The conceptual design process of ika is visualized in Figure 1 in the form of a V-diagram.
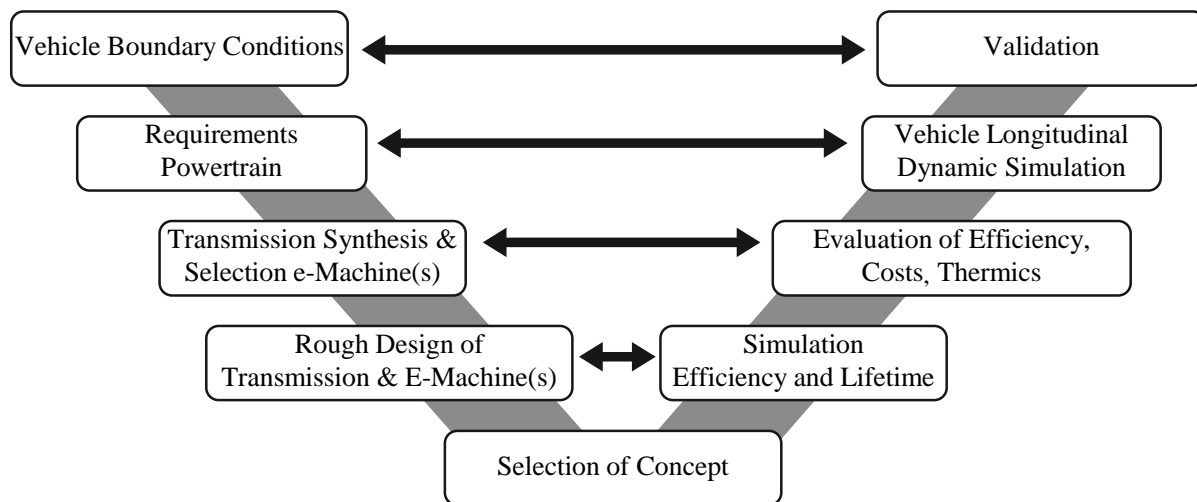

Figure 1: V-model of the ika design methodology for electric powertrains

In the subsequent step of the design process, possible topologies of the powertrain and transmission are generated. These are evaluated using a longitudinal dynamic vehicle model. Predefined criteria are used for evaluation, including the system's complexity, the achievable driving performance and the number of system elements. The most promising topologies according to these criteria are then further detailed. The shaft-bearing system is first defined in this detailing, and an initial design of the basic gearing parameters is carried out. This enables a component-based efficiency calculation of the concepts whereby a well-founded second evaluation and prioritization of the remaining topologies can be carried out. Based on this efficiency simulation, a thermal node model of the gearbox is created automatically. This model assigns the losses calculated for each component to the thermal nodes of the respective components and links them to each other according to the gearbox configuration. In addition, a simplified gearbox housing is generated to calculate heat dissipation to the environment. The gear oil, which plays a decisive role in heat transfer, is also considered in this method. An approach based on particle simulations was developed to integrate the oil into the thermal model presented in the publications by Köller et al. and Uerlich et al. [8,9]. Since this paper focuses on validating the models using measurement data, we refer to the mentioned publications for a detailed elaboration of the modelling process.

2.1 Requirements Specification based on VECTO

The urban delivery cycle of VECTO was chosen as the basis for this design process in the exemplary application for the 'Concept-ELV²' project. As there is currently no modification of this cycle for battery electric vehicles integrated in VETCO, the cycle of conventionally powered vehicles was used for the evaluation. This driving cycle is shown in Figure 2. [1]
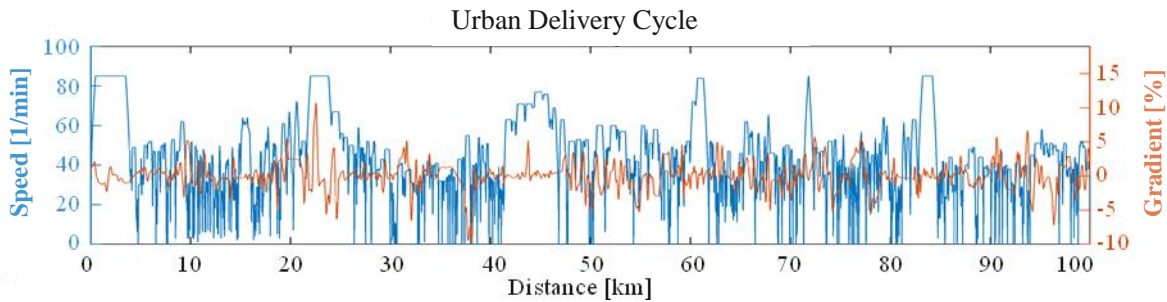

Figure 2: Urban Delivery Cycle of VECTO [1]

The diagram shows the required speeds in blue and the gradients in orange. It can be seen that the urban delivery cycle involves comparatively few constant-speed sections, but rather continual acceleration and braking demands. In addition, a wide range of road gradients is taken into account. This results in a set of requirements which, due to the homogeneous distribution of driving conditions within the cycle, delivers significantly more complex requirements in terms of overall vehicle efficiency.

2.2 Methodical Approach for the Automated Identification of Suitable Powertrain Topology and Gearbox Design

The processing of these requirements is carried out according to a method presented in detail in the work of Köller et al. [10]. The method introduced there differs from other state-of-the-art methods in its holistic approach to identifying solutions and subsequent optimization. In addition, the degree of automation sets it apart from other prior art processes and enables a large solution space of possible topologies to be included in the approach. The three essential design steps of topology synthesis, initial gear dimensioning, and evolutionary combination are carried out within the method.

In the topology synthesis, all possible transmission topologies are generated that comply with the driving requirements and the restrictions of the solution space, such as the maximum number of gear stages, required torque and maximum speed. For these topologies, an estimation of the characteristic gearing parameters is conducted already in the first development step, allowing prioritization of the topologies according to their fitness. For this purpose, the criteria complexity, costs, and efficiency are assessed based on the limited number of available parameters. The second step is followed by an initial dimensioning of the gear elements for the most promising variants. This analytical process is based on ISO 21771 and ISO 6336 [11,12]. Through the analytical approach, a large number of gear variants are considered and optimized in the final step of the method with the help of a genetic algorithm. This algorithm weights and combines the solution variants concerning system mass, safety, lifetime and efficiency. The user determines the importance of these criteria according to the application's requirements. In the context of the application within the 'Concept ELV²' project, 10^9 gearbox variants were initially generated with this algorithm, of which about 400 variants were dimensioned in a second step. A selection of these variants and the prototypically realized variant is shown in Figure 3.
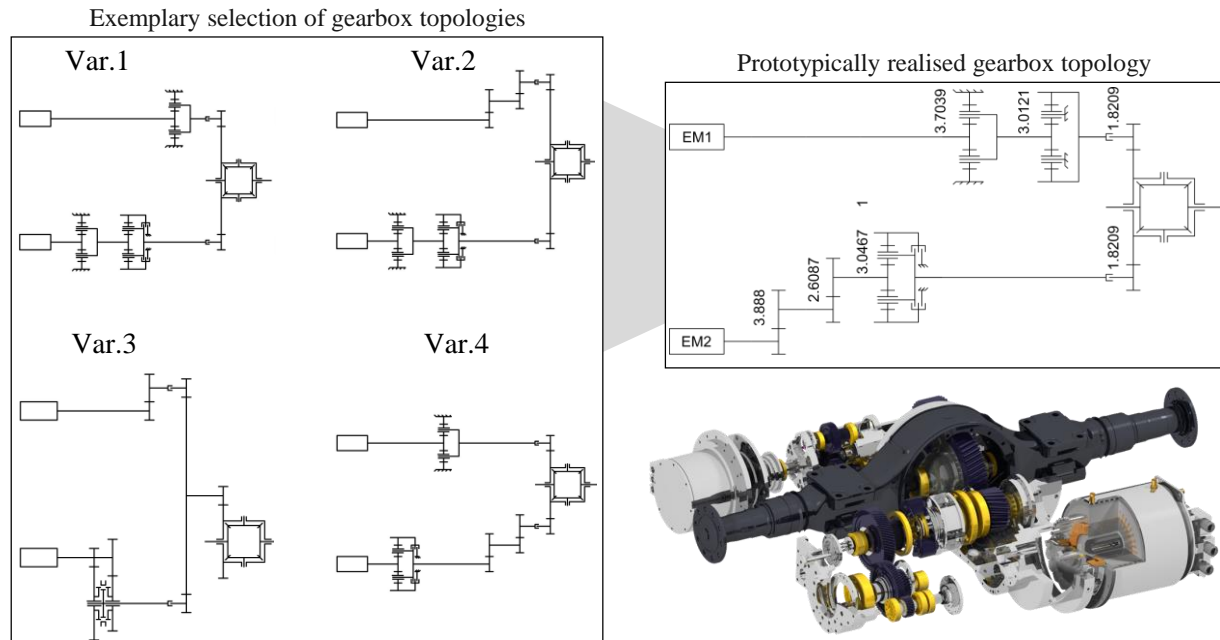
Figure 3: Exemplary selection of considered gearbox topologies and representation of the selected topology of the gearbox prototype as well as its realization in CAD [8,9]

The selection of gearbox topologies shown here provides a small insight into the bandwidth. In all transmission topologies, two electric machines were set as a boundary condition, as these should ensure more efficient coverage of the widely varying load requirements of a heavy commercial vehicle. In variant 1, mainly planetary stages are used to realize the transmission, whereas in variant 3 only spur gear stages are used. Variant 2 and variant 4 represent different combinations of these gearing elements, so the advantages of both element types can generate an advantage in terms of service life or efficiency in one system. In addition to the automated weighting, the selection of the realized topology was based on the aspects of manufacturability and research-relevant system designs. Thus, a stepped planet was designed for electric machine one and a shiftable planetary stage with decoupled through-drive for electric machine two. A detailed presentation of this concept has been given in Uerlich et al. [8].

2.3   Method of Iterative Efficiency Simulation

An iterative calculation of the component losses is subsequently carried out for the generated and top-rated gearbox topologies for in-depth evaluation of the concepts. Based on the initially defined overall structure, it is necessary to determine the shaft-bearing system and specify the bearing positions as well as the gear configuration. The general sequence of the process is divided into the modelling of the gearbox components bearings, shafts and gears, followed by linking those to each other with elements like gear pairs and couplings. After the complete modelling of the mentioned components, the system of equations is set up automatically for each topology treated. In these, the speed relationships and the force and torque flows within the system are taken into account. In the first solution step, this equation system is solved without considering the system losses. These are then determined iteratively in a subsequent calculation step. The resulting losses lead to a load reduction for the following elements in the torque flow. Hence the iterative consideration is necessary. This process was presented comprehensively in the publication by Kieninger et al. and further publications by Köller et al. and Uerlich et al. and is therefore not explained in depth here [7,8,10]. The results of this calculation approach for the designed topology of the 'Concept-ELV²' project are shown in Figure 4 for the switchable transmission part of the electric machine two (EM2).
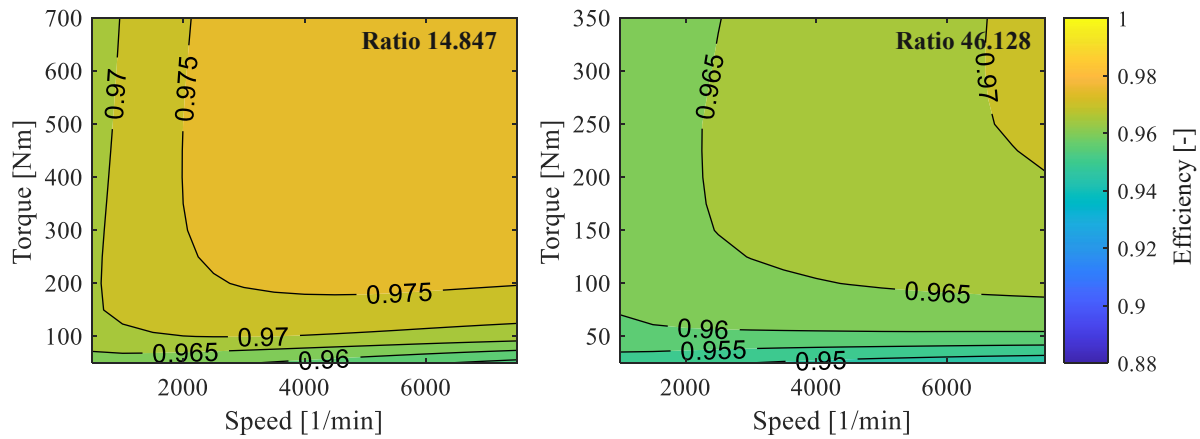
Figure 4: Simulative efficiency maps of the switchable gear stage of the EM2 from Concept ELV²

The addition of the planetary stage causes a reduction in the overall efficiency of about one percent over the entire map. This influence is comprehensible due to the increased number of tooth contacts generated by the addition of the planetary stage and corresponds to the expectations based on known literature values [13]. Drag losses are neglected in the loss calculation, as no approach for the early stage of the gearbox design could be identified that would allow a feasible estimation. The gear losses calculated for each component are used in the following process step for the thermal assessment of the gearbox concept.

2.4   Thermal Modelling Approach

Within ISO/TR 14179-2 [14], an approach for calculating the gearbox temperature is introduced, which relates the power loss of the gearbox to the outer surface of the housing. With this method, a thermal equilibrium state is calculated for the gearbox. This approach is not possible to identify thermally critical system parts due to the simplified procedure. The procedure also provides only limited information, as the standard already pointed out that a deviation of 14 % from measured values is to be expected. To be able to make a more precise prediction, a thermal network is generated for the gearbox at this point in the ika method, which includes at least three nodes for each loss-generating gearbox component. An exemplary network of a gearbox section is shown in Figure 5. In this figure, the meshing of the bearings, gears, shaft, seal, housing, oil and environment can be traced on a gearbox section.
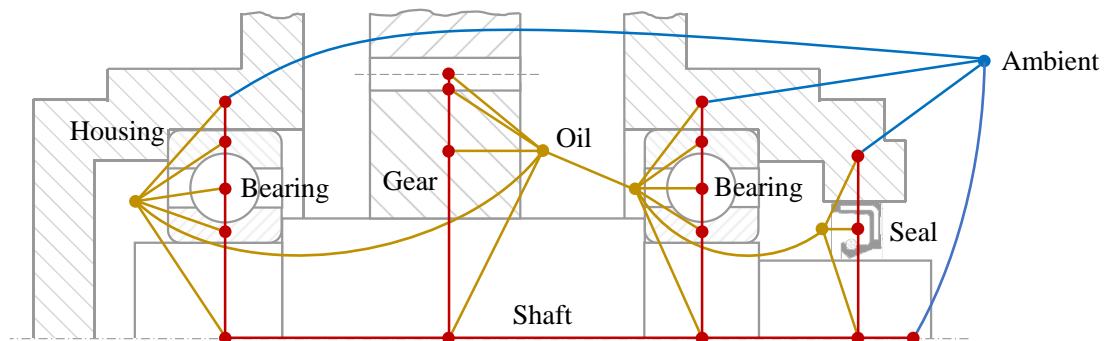

Figure 5: Exemplary representation of the thermal node model for a gearbox section

The thermal modelling approach of a gear using thermal networks is already established. Such an approach was already used by Blok [15] to model a single-stage FZG gear test rig. This modelling aimed to obtain feedback on the thermal behaviour of the tooth contact, the lubricant film in the tooth contact and the tooth flank. This modelling approach was not validated by measurement in his work and used a too coarse mesh with five accounts.

In Funck's [16] work, this approach was refined and validated by measurement. However, a deviation of 25 % between the measured value and the model was determined there.

A significant improvement in the results was achieved by Geiger [17], who further refined the thermal network and divided the gear into thermal nodes tooth flank, tooth body and gear wheel. Similarly, the shafts were divided into several nodes. The gear oil was still represented as one node at this point, which can be considered sufficient due to the structure of an FZG test rig. Additionally, his work implemented an approach that enables temperature calculation under transient load conditions. With these adjustments, good compliance between the model and the measurements was achieved, with a deviation of about 10 %.

The approach used in this paper is based on the previously mentioned approaches but differs in the chosen application. Instead of a single-stage FZG test rig, multi-stage vehicle gearboxes are modelled. These vary not only in the number of stages but also in the housing design. A more closely fitting form is assumed for vehicle transmissions instead of the cuboid housing shape used in the FZG test rig. In this approach, an automatically generated housing is created based on the shaft arrangement and corresponds to a detailed housing only as an initial approximation. The interior of the housing, which is also modelled in this way and filled with an oil-air mixture during operation, is subdivided into further sub-elements and represented with a thermal node for each. This subdivision enables thermally critical points within the gearbox to be identified based on the oil node temperatures. The gears in the model consist of the nodes flank, tooth and gear body and bearings are represented by the nodes inner ring, rollers, and outer ring. The shafts are divided into smaller shaft segments. The calculation procedure is divided into four essential steps: generation of the thermal network, time-step calculation, temperature calculation and evaluation. These steps and their details are shown in a flow chart in Figure 6.
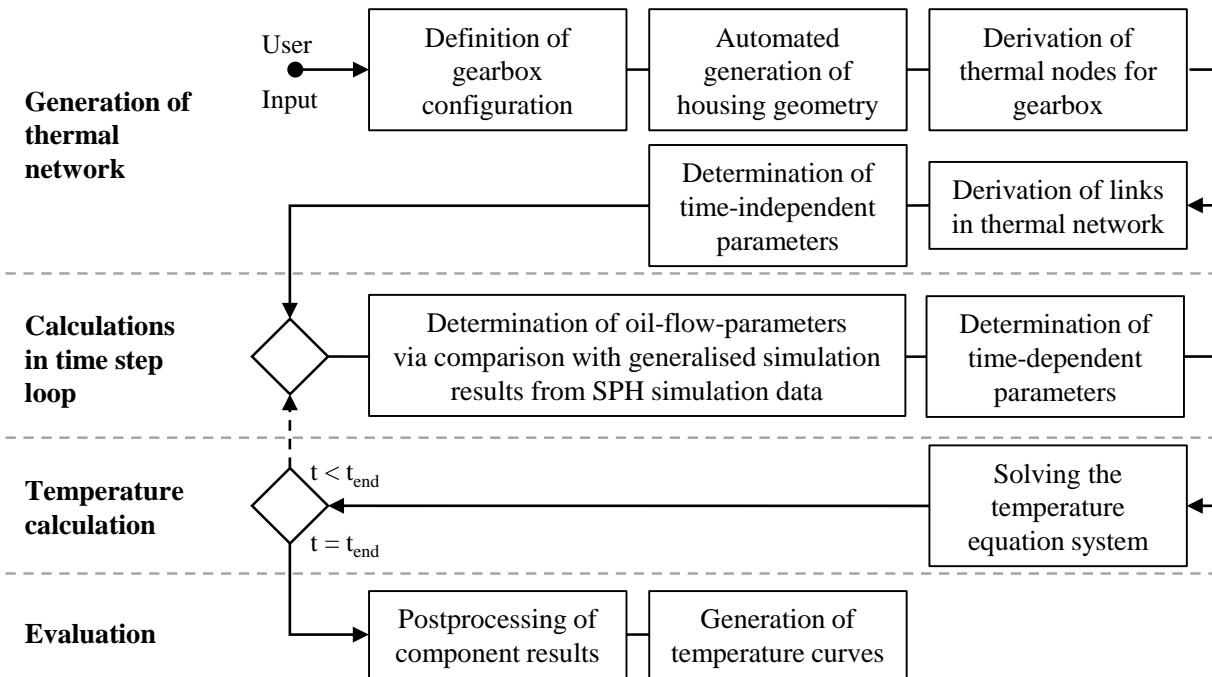

Figure 6: Stepwise process of model generation and calculation of the thermal network

First, the gearbox components are divided into single nodes and required data is specified and determined. After automatically detecting all links between the nodes, the time-independent parameters are calculated. In step two, the time-dependent parameters and conductivity values are determined. Also, the flow state of oil is calculated based on look-up tables from SPH simulations. The next step is solving the equation system for the component temperatures for the respective time step using the calculated parameters before. In the final step, the results of the component-by-component calculation are combined and evaluated.

3   Results

The measurement results of the prototype gear unit are presented in the following and used to validate the simulation results. For the measurement, the gear unit was mounted between test bench machines. These emulated the electric motor as the drive unit on the one hand and the output on the wheel on the other. The mechanical efficiency was determined using a torque measurement sensor at the gearbox input and a torque measurement sensor at the gearbox output.

3.1   Efficiency results

The gearbox efficiency maps of Figure 7 were recorded with this measurement setup. These maps show the system's efficiency concerning the input speed and the input torque. Both maps show gaps in the upper speed and torque range compared to the simulation. These ranges have not been measured since the driving requirements do not demand them of the vehicle and could not be covered using the emulated electric motor. Furthermore, these areas were not considered in the in-depth design of the gearbox, as this would lead to a massive over-dimensioning of the unit compared to the requirements.
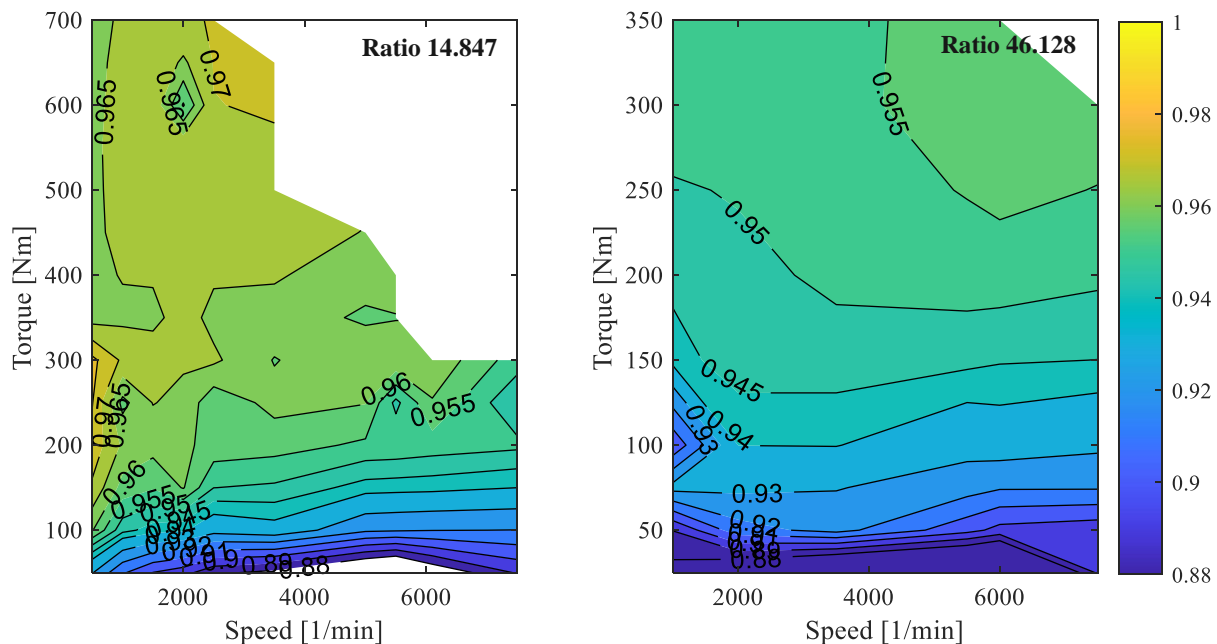

Figure 7: Measured efficiency maps of the prototype electric drive axle

Compared to the simulation, there is a deterioration in efficiency of one to two percent in both gears in the range above 150 Nm input torque and over the entire speed range. Below this input torque, this deviation increases for the gear with the transmission ratio of 14.847 to five percent at 100 Nm and up to ten percent in torque-free operation. This is the same as for the gear with a ratio of 46.128, but a five percent deviation only occurs at an input torque of 75 Nm and a ten percent deviation during towing operation. These slight deviations can be attributed to the changed speeds caused by the different gear ratios, especially since the load-independent losses significantly influence the efficiency in these load ranges. Thus, the comparatively high deviation of the measurement results in the lower efficiency map range is largely due to the lack of modelling of the drag losses, the implementation of which is currently still a current research topic point.

3.2   Thermal Modelling and Measurement Results

Alongside the efficiency measurement of the gearbox, a thermal characterization was also carried out. For this purpose, the load cases listed in Table 1 were recorded in a steady state. Each of these load cases was held for

30 minutes. Then the gearbox was cooled down to its initial state so that the measurement of the following load case could be carried out with approximately the same initial state. However, slight deviations due to different initial temperatures of the individual cannot be avoided due to the test setup.

Input torques of 100, 200 and 300 or 400 Nm were run in both gears, depending on the total power applied. For the gear with a ratio of 14.847, input speeds of 2500, 5000 and 7500 rpm were used to represent the wide range of driving speeds of this gear. In gear with the ratio of 46.128, which was designed for the starting manoeuvres, only 2500 and 7500 rpm were used as engine speeds, as this gear only covers a comparatively lower speed range. The inlet of the injected oil was always kept at a constant 50 °C so that its influence as the primary heat transporter could be specifically demonstrated. For this purpose, the injection temperatures were changed to 40 °C and 60 °C at individual load points. This also allowed the influence on the inertia of the thermal system to be traced.

Table 1: Overview of load cases that were carried out on the test bench

Gear Ratio	Rot. Speed [1/min]	Torque [Nm]	Oil Temp. [°C]	Gear Ratio	Rot. Speed [1/min]	Torque [Nm]	Oil Temp. [°C]
14.847	2500	100	40, 50, 60	46.128	2500	100	50
	2500	200	40, 50, 60		2500	200	40, 50
	2500	400	50		2500	300	50
	5000	100	50		7500	100	50
	5000	200	40, 50, 60		7500	200	40, 50, 60
	5000	400	40, 50, 60		7500	300	40, 50
	7500	100	50				
	7500	200	40, 50, 60				
	7500	300	50				

Figure 8 shows the result of such a thermal characterization for the load case 5000 1/min input speed 400 Nm input torque and 50 °C oil injection temperature in gear with the transmission ratio 14.847 and its simulation superimposed. In this illustration, the three thermal accounts of a bearing inner ring, a gear tooth, and a housing segment for the second gearbox shaft are shown. When designing the prototype, the integration of temperature sensors in the rotating gearbox elements for their thermal measurement was feasible in this shaft due to the gearbox layout.
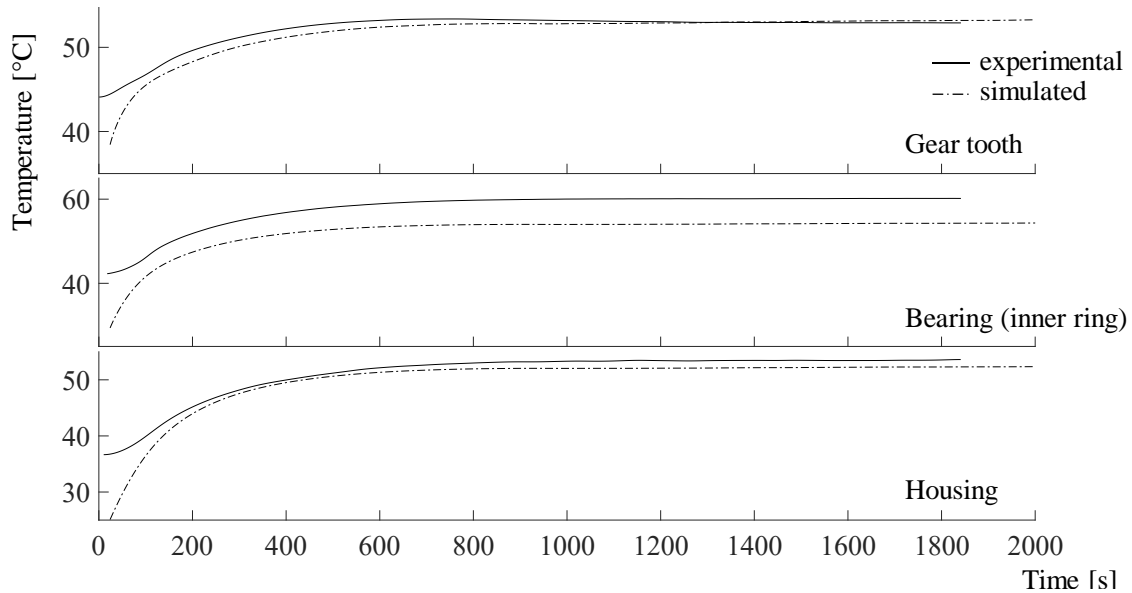

Figure 8: Comparison of temperature curves for a gear tooth, an inner ring of a bearing and a housing segment

While the end temperature deviation of the bearing is about ten degrees celsius, the simulated temperatures of the gear tooth and the housing segment show good accordance with the measured temperatures. Since the gearbox was not always cooled down to the ambient temperature between test runs, there are more significant temperature differences for $0\,\text{s} \leq 100\,\text{s}$. To derive a statement about the thermal inertia of the system despite this transient, the gradient of the temperature increase was introduced as an evaluation variable and is shown in Figure 9.
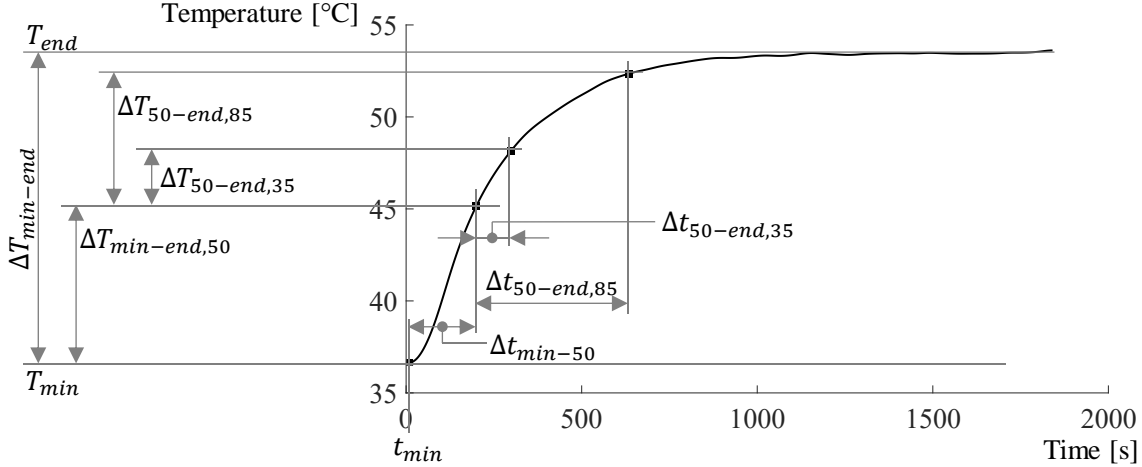

Figure 9: Key temperature and time parameters

However, since the first 100 s of the measured values are needed for the system to stabilize, the time when the system has already reached 50 % of the final temperature is selected as the starting point. Starting from this point, the gradients for 35 % and 85 % of the remaining 50 % are determined according to equation (1) - (6). These are evaluated as characteristic values in the following.

An average value of the last five percent of the test time is chosen as the final temperature for this calculation to not give too much weight to any measurement deviations of a single measuring point. The minimum system temperature results in the initial temperature delta according to equation (1).

$$\Delta T_{min-end} = T_{end} - T_{min} \tag{1}$$

Subsequently, the final temperature differences are determined:

$$\Delta T_{min-end,50} = 0.5 \cdot (T_{end} - T_{min}) \tag{2}$$

$$\Delta T_{50-end,35} = 0.35 \cdot \Delta T_{min-end,50} \tag{3}$$

$$\Delta T_{50-end,85} = 0.85 \cdot \Delta T_{min-end,50} \tag{4}$$

The characteristic time intervals are then calculated by:

$$\Delta t_{50-end,35} = t\left(T_{min} + \Delta T_{min-end,50} + \Delta T_{50-end,35}\right) - t\left(T_{min} + \Delta T_{min-end,50}\right) \tag{5}$$

$$\Delta t_{50-end,85} = t\left(T_{min} + \Delta T_{min-end,50} + \Delta T_{50-end,85}\right) - t\left(T_{min} + \Delta T_{min-end,50}\right) \tag{6}$$

The key temperature parameter and the key time parameters are equally calculated for the simulation. For example, if the measured temperature course is steeper than the simulated, the key time intervals are shorter for the measurements than for the simulations. Figure 10 illustrates the comparison of the final temperatures between simulation and experiment in the left-hand diagram, while the right-hand graph shows the inertia based on the time interval for reaching $\Delta t_{50-end,35}$ and $\Delta t_{50-end,85}$. The system temperatures show good agreement with a deviation of less than ten percent on average, of the final temperatures, with the maximum deviations of single data points going up to 50 %. This diagram also shows that the simulated temperatures tend to be lower than the

measured ones. On the one hand, this is due to the detailed design of the housing and its surrounding airflow and, on the other hand, to the already proven deviations of the loss modelling. A further source could be the thermocouples used, which have a relatively high measuring deviation compared to the measuring range with a tolerance of 1.5 K.
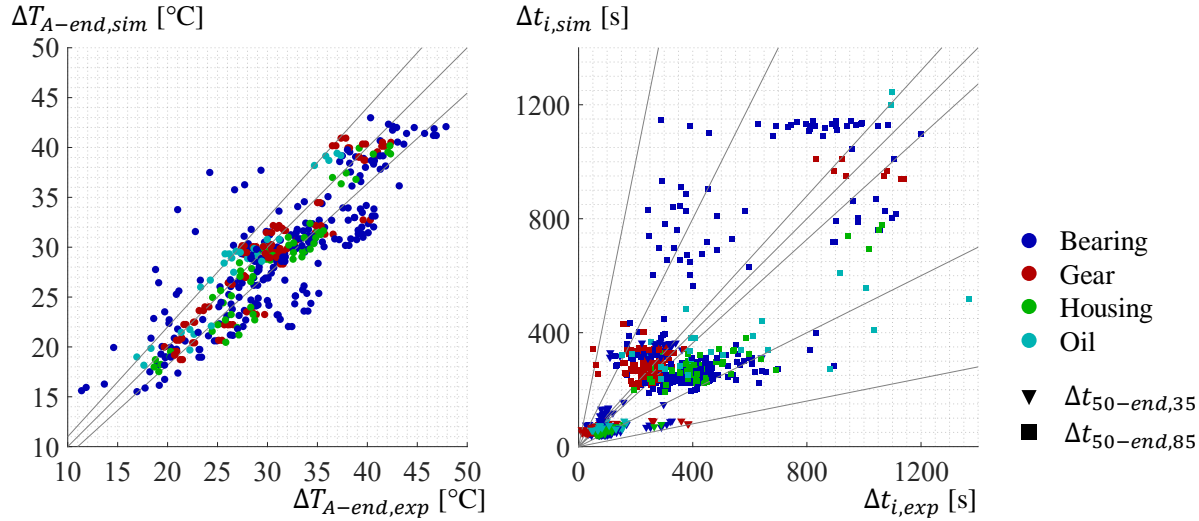

Figure 10: Comparison of simulated key parameters versus measured key parameters for all load cases in table 1

The inertia of the system shows a broader scatter, which can be attributed on the one hand to the chosen approach of the slope evaluation or to the relatively short time interval considered in this approach. This result is superimposed by the good alignment of the temperature curves of the respective components. To determine the system inertia in a later evalutaion step a longer time interval and a more detailed gearbox configuration will be considered. The work focused fundamental evaluation of the modelling could already be demonstrated despite this deviation.

4   Conclusion & Outlook

In this paper, an overview of the validation of the method developed at Institute for Automotive Engineering (ika) to evaluate transmission concepts was given. In the assessment of the loss modelling, it was shown that even with the limited information available, a sufficiently good approximation of the measured losses could be given. The drag losses, which have been neglected, were only noticeable in areas of comparably low system performance. The evaluation of the thermal system properties based on this loss modelling was also able to provide a good approximation, particularly concerning the stationary end temperatures of the system. Deviations of a few degrees between the simulation model and the measurement were noted here. This is a promising result, especially considering the highly simplified housing within the simulation model, and thus provides a good supplement in identifying thermally critical system points. The evaluation of the thermal inertia, on the other hand, is afflicted with more significant deviations. In addition to the deviating housing design and the associated deviating thermal mass of the housing, deviations in the thermal masses of the shafts and gears due to the CAD design must also be considered as possible causes.

Recalculating the thermal model by scaling the loss components to the level of the measured losses led to a further improvement in the forecast for the final temperatures. The system inertia was also significantly improved by adjusting the thermal masses according to the CAD models. Thus, the function of the approach could be proven, but the use case of an early system evaluation does not allow such a system adaptation for the large number of systems considered. In summary, the loss calculation and the identification of the thermally critical components provide good results and the modelling can therefore be considered validated for the application within the 'BEV Goes eHighway - [BEE]'. Consequently, valuable predictions of the vehicle characteristics can be derived for a large number of powertrain configurations.

Acknowledgements

References

1. European Parliament and Council. *REGULATION (EU) 2019/1242 OF THE EUROPEAN PARLIAMENT AND OF THE COUNCIL*: *setting CO2 emission performance standards for new heavy-duty vehicles and amending Regulations (EC) No 595/2009 and (EU) 2018/956 of the European Parliament and of the Council and Council Directive 96/53/EC*; Official Journal of the European Union: Brüssel, 2019.

2. ACEA. *CO2 emissions from heavy‑duty vehicles*: *Preliminary CO2 baseline (Q3‑Q4 2019) estimate*: Brüssel, 2020.

3. Rodríguez, F. *The Future of Vecto*: *CO2 Certification of Advanced Heavy-Duty Vehicles in the European Union*, 2019.

4. Fiori, C.; Ahn, K.; Rakha, H.A. *Power-based electric vehicle energy consumption model: Model development and validation*, 2016.

5. Earl, T. *Analysis of long haul battery electric trucks in EU*: *Marketplace and technology, economic, environmental, and policy perspectives*: Graz, 2018.

6. Kieninger, D. *The highly integrated ModulED drive module – Holistic concept design*, 2020.

7. Kieninger, D.; Hemsen, J.; Köller, S.; Uerlich, R. Automated Design and Optimization of Transmissions for Electric Vehicles. *MTZ Worldw* 2019, *80*, 88–93.

8. Uerlich, R. *Concept ELV² Design of an Electric Drive Axle for Heavy Distribution Traffic*: Aachen, 2021.

9. Köller, S.; Uerlich, R.; Witham, G.; Eckstein, L. Concept ELV² – Development of an Electric Drive Axle for Heavy Commercial Vehicles. In *ELIV 2021*: VDI Verlag, 2021, 653-XVI.

10. Köller, S.; Schmitz, V. *Systematic synthesis and multi-criteria evaluation of transmission topologies for electric vehicles*, 2021.

11. *DIN ISO 6336:2019,Calculation of load capacity of spur and helical gears (ISO_6336:2019)*; Beuth Verlag GmbH: Geneva.

12. *DIN ISO 21771:2014-08, Zahnräder_- Zylinderräder und Zylinderradpaare mit Evolventenverzahnung_- Begriffe und Geometrie (ISO_21771:2007)*; Beuth Verlag GmbH: Berlin.

13. Naunheimer, H.; Bertsche, B.; Ryborz, J.; Novak, W.; Fietkau, P. *Fahrzeuggetriebe*; Springer Berlin Heidelberg: Berlin, Heidelberg, 2019.

14. ISO/TC 60/SC 2. ISO/TR 14179-2:2001: Gears — Thermal capacity — Part 2: Thermal load-carrying capacity 2001.

15. Blok, H. Recent Developments in Gear Tribology. *Proceedings of the Institution of Mechanical Engineers* 1969.

16. Funck, G. Wärmeabführung bei getrieben unter quasistationären Betriebsbedingungen: Dissertation, TU München 1985.

17. Geiger, J. Wirkungsgrad und Wärmehaushalt von Zahnradgetriebem bei instationären Betriebsbedingungen: Dissertation, TU München 2014.

Authors

Roland Uerlich studied mechanical engineering with a major in development and design at RWTH Aachen University. After graduating, he began his professional career at the Chair of Design Engineering at Braunschweig Technical University. There he started his PhD in battery system development and then took over the role of team leader within the institute working group. Since January 2019 he has been working at the Institute for Automotive Engineering (ika) at RWTH Aachen University. He has been group leader Drivetrain Systems there since end of 2019. After working on the development of the concept and prototype of the electrified drive axle of the 'Concept ELV²' project, he is coordinator of the 'BEV Goes eHighway – [BEE] ' project since 2022.

Sven Köller studied mechanical engineering with a major in Automotive Engineering at RWTH Aachen University. After his graduation, he joined the Institute for Automotive Engineering (ika) at RWTH Aachen University to start his PhD in 2018. He is part of the institutes' drivetrain department. His research focuses on developing holistic methods to design transmissions in electrified powertrains. Within the 'Concept-ELV²' project, he was responsible for the design of the gearbox topology and also contributed to its prototypical realisation. Besides the research aspects, he supervises 'Automotive Engineering I' course. Additionally, he started his MBA-studies in 2020.

Gordon Witham studied mechanical engineering with a major in Automotive Engineering at RWTH Aachen University. After his graduation, he joined the Institute for Automotive Engineering (ika) at RWTH Aachen University in the Energy Management & Drivetrains department to start his PhD in 2019. His research focuses on the conception and optimization of battery-electric drive systems, for which he has contributed to the EU-funded project 'ModulED - Modular Electric Drivetrains' as work package and project leader. Besides research, he supervises the lecture 'Alternative and Electrified Vehicle Propulsion Systems'.

Theo Koch is studying mechanical engineering with a major in Automotive Engineering at RWTH Aachen University. After his bachelor's thesis, which dealt with the thermal balancing of gearboxes, he pursued this topic as a student researcher at the Institute for Automotive Engineering (ika). There he is part of the drivetrain department, and his work concentrates on expanding the thermal modelling of gearboxes.

Lutz Eckstein is the director of the Institute for Automotive Engineering (ika) at RWTH Aachen University. The institute has more than 160 employees and spans its research scope widely across all vehicle-related fields: Electronics, chassis, body, drivetrain, thermal management, acoustics, autonomous driving, future vehicle concepts and -strategy. Furthermore, he is chairman of the Advisory Board of fka GmbH, chairman of the 'VDI Advisory Board Vehicle and Traffic Technology', and a member of SAE. Additionally, he is active as a member of Member of the Board of Academic Advisers to the Federal Minister of Digital and Transport